frontiers | Frontiers in Marine Science

TYPE Original Research
PUBLISHED 15 November 2024
DOI 10.3389/fmars.2024.1499109

OPEN ACCESS

EDITED BY
Qing Wang,
Chinese Academy of Sciences (CAS), China

REVIEWED BY
Lin Zhu,
Chinese Academy of Fishery Sciences (CAFS), China
Zongling Wang,
Ministry of Natural Resources, China

*CORRESPONDENCE
Shunxin Hu
hushunxin001@163.com

†These authors have contributed equally to this work and share first authorship

RECEIVED 20 September 2024
ACCEPTED 21 October 2024
PUBLISHED 15 November 2024

CITATION
Zhang Y, Liu C, Li B, Chen L, Xiang Z, Tian X, Sun C, Gao J, Qiao R and Hu S (2024) Mechanisms of ROS-induced mitochondria-dependent apoptosis in *Phaeodactylum tricornutum* under AgNPs exposure. *Front. Mar. Sci.* 11:1499109. doi: 10.3389/fmars.2024.1499109

Mechanisms of ROS-induced mitochondria-dependent apoptosis in *Phaeodactylum tricornutum* under AgNPs exposure

Yunfei Zhang[1,2,3†], Caili Liu[1,2†], Bin Li[1,2], Lizhu Chen[1,2], Zhiwei Xiang[1,2], Xiuhui Tian[1,2], Chunxiao Sun[1,2], Jiqing Gao[1,2], Ruiguang Qiao[1,2] and Shunxin Hu[1,2*]

[1]Shandong Marine Resource and Environment Research Institute, Shandong, Yantai, China, [2]Shandong Marine Ecology Restoration Key Laboratory, Shandong, Yantai, China, [3]College of Fisheries and Life Sciences, Shanghai Ocean University, Shanghai, China

Introduction: Nanomaterials such as silver nanoparticles (AgNPs) have gained widespread application across various fields. However, the large-scale production and application of AgNPs have raised concerns about their distribution in the environment and potential pollution issues.

Methods: This study investigates the toxic effects of AgNPs on the diatom *Phaeodactylum tricornutum* by employing electron microscopy for cellular observation, quantifying apoptotic cell numbers, and measuring antioxidant indicators. The research examines how varying concentrations of AgNPs induce stress in *P. tricornutum* and the specific mechanisms of the toxic effect.

Results: The findings reveal that AgNPs induce apoptosis in *P. tricornutum* cells by triggering a mitochondria-mediated pathway, marked by a decrease in mitochondrial membrane potential and the activation of caspase enzymes. Additionally, AgNP exposure results in an overproduction of reactive oxygen species (ROS) within the algal cells, leading to lipid peroxidation of the cell membrane and a consequent increase in malondialdehyde (MDA) levels. This oxidative stress response induces the upregulation of antioxidant enzyme activities in an attempt to mitigate the excessive ROS.

Discussion: ROS is identified as the primary factor responsible for inducing mitochondria-mediated apoptosis. The research results will provide a theoretical basis for understanding the toxic effects and mechanisms of AgNPs on marine microalgae.

KEYWORDS

***Phaeodactylum tricornutum*, silver nanoparticles, apoptosis, oxidative stress, ecotoxicology**

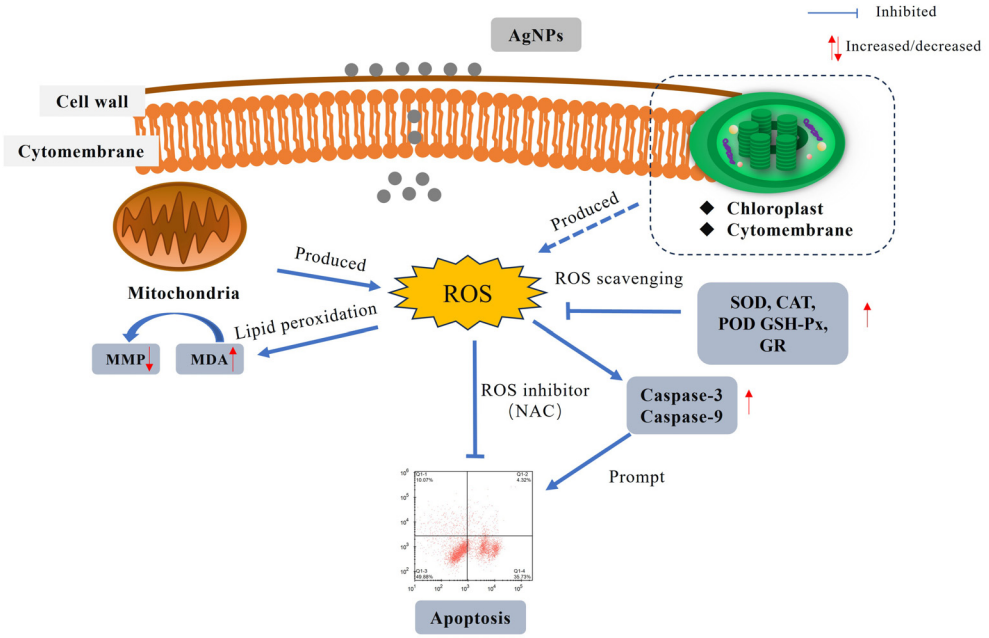

GRAPHICAL ABSTRACT

1 Introduction

In recent years, nanomaterials have been widely used in various fields such as medicine, cosmetics manufacturing, and emerging energy due to their small particle size, which imparts unique properties such as surface and interface effects, and quantum size effects (Cui et al., 2014; Hong et al., 2014; Atta et al., 2015). Silver nanoparticles (AgNPs), among the most widely used nanomaterials, are recognized in the aquaculture industry as a potential alternative to antibiotics due to their exceptional antibacterial properties. They are frequently employed for water sterilization and the prevention of fish diseases during the aquaculture process. However, with the increasing use of products containing AgNPs, the environmental levels of AgNPs have been steadily rising (Zhao, 2018). AgNPs are released into the environment through various means such as production, transport, and consumption (Chinnapongse et al., 2011). This has directly contributed to the increase in AgNPs levels in the environment, ultimately accumulating in aquatic systems such as oceans and lakes, posing a threat to the ecological environment (Tortella et al., 2023).

With the widespread use of AgNPs, the concentration of AgNPs in water bodies has increased. By 2020, measured AgNPs concentrations in water have reached 0.01mg L^{-1} (Huang et al., 2020). Upon entering the aquatic environment, AgNPs stimulate the organism to produce large amounts of reactive oxygen species (ROS) (Qu et al., 2023). Subsequently, they damage biomolecules such as lipids, proteins, and nucleic acids, disrupting cellular metabolism (Xuerong et al., 2018). After entering the organism, AgNPs bind to DNA (Zheng and Wang, 2021), disrupting transcription and replication processes, which leads to DNA damage and subsequently affects cell division. AgNPs can also impact the structure and permeability of cell membranes (Subaramaniyam et al., 2023), ultimately causing cell apoptosis.More and more studies indicate, nanomaterials can induce stress in marine organisms, leading to oxidative stress and disrupting cellular metabolism, ultimately resulting in cell death (Campbell et al., 2019). Current research indicates that the impact of nanomaterials on the antioxidant system of Nile tilapia (*Oreochromis niloticus*) primarily manifests in the occurrence and intensity of oxidative stress. AgNPs and Titanium dioxide nanoparticles dioxide can induce an increase in the activity of antioxidant enzymes such as superoxide dismutase and glutathione peroxidase in the liver cells of fish, thereby reducing the degree of oxidative stress (Mansour et al., 2021). The effects on blue mussels (*Mytilus edulis*) are also mainly focused on oxidative stress levels, where aluminum oxide nanoparticles and Titanium dioxide nanoparticles can affect the activity of redox enzymes and antioxidant enzymes in the liver and gill tissues of mussels, resulting in aggravated oxidative stress (Châtel et al., 2018). In the case of wild cherry shrimp (*Neocaridina denticulata*), AgNPs can protect them from oxidative stress damage by increasing the activity of antioxidant enzymes such as superoxide dismutase and glutathione peroxidase (Pu et al., 2021). Comparatively, in high concentrations and prolonged exposure (ranging from 14 to 28 days), fish exhibit oxidative stress reactions in the initial days, but with increasing exposure time, a certain degree of recovery is observed (Johnson et al., 2022; Parker et al., 2024). Presently, research on AgNPs is mostly focused on cultured fish, crustaceans, and similar species. Studies by Dash (Dash et al., 2012) have shown that AgNPs can inhibit chlorophyll synthesis in *Chlorella vulgaris*, while research by El-Kassas (Elsheekh and Elkassas, 2014) found that AgNPs suppress the survival of *Microcystis aeruginosa*. The impact of AgNPs on the antioxidant system of *Chlorella vulgaris*

primarily manifests in the incidence and intensity of oxidative stress. Nanomaterials such as AgNPs and nano-TiO2 (Vicari et al., 2018; Jun, 2016) can induce increased activity of antioxidant enzymes, including superoxide dismutase and glutathione peroxidase, in algal cells, thereby reducing the extent of oxidative stress. Similarly, their effect on *Microcystis flos-aquae* (Zong et al., 2022) is largely concentrated on oxidative stress levels. AgNPs also affect the activity of oxidoreductase and antioxidant enzymes in *Dunaliella salina* (Hassanpour et al., 2021), exacerbating oxidative stress. In studies on *Microcystis aeruginosa* (Huang et al., 2023), AgNPs were found to protect the cells from oxidative stress by increasing the activity of antioxidant enzymes, such as superoxide dismutase and glutathione peroxidase. However, there is still a need for in-depth exploration regarding the antioxidative mechanisms and cell apoptosis induced by AgNPs in microalgae.

Diatoms, as a significant component of marine algae, constitute more than 60% of marine planktonic organisms (Chen et al., 2006). They play a vital role in marine ecosystems and are among the primary participants in the carbon cycle. Due to their rich content of proteins, polysaccharides, vitamins, and other nutrients, as well as their ease of cultivation, diatoms are commonly used as feed materials (Yue, 2010). *Phaeodactylum tricornutum*, as a typical diatom, is frequently used as a model organism in research related to ecology, genetics, biogeochemistry, and other fields. This experiment investigates the toxic effects of AgNPs on marine diatoms by measuring antioxidative enzymes and related products, cell apoptosis, and changes in cell membrane potential. The research results will provide a theoretical basis for understanding the toxic effects and mechanisms of AgNPs on marine microalgae. Moreover, it will support the objective evaluation of the safety and ecological risks of AgNPs as antibacterial agents in aquaculture.

2 Materials and methods

2.1 Microalgae cultures

P. tricornutum, provided by the Algal Center of the Laboratory of Marine Ecology at Ocean University of China, was cultured in 500 mL conical flasks containing 300 mL of sterile seawater supplemented with f/2 medium (Qu et al., 2023). The flasks were incubated in a temperature- and light-controlled chamber set to 20 ± 1°C with a light intensity of 65 μmol·m^{-2}·s^{-1}, following a 12 h light/12 h dark cycle. To prevent microalgal cells from settling at the bottom, the cultures were gently shaken twice daily. Algal cells in the exponential growth phase were then used to inoculate fresh culture media for the toxicity experiments. Seawater was collected from the coastal waters near Yantai City, filtered through a 0.45 μm membrane, sterilized at 121°C for 15 minutes, and cooled to room temperature before use.

According to the results of the pre-experiment and with reference to the environmental concentrations, five exposure concentration groups were established in the experiment: 0 (control), 0.01 (ambient concentration), 1, 2, and 4 mg L^{-1} (Huang et al., 2020).

2.2 Experimental design and sample analysis

The nominal AgNPs concentrations in the seawater were achieved by adding the appropriate amount of a AgNPs stock solution (5 g L^{-1}) to the experimental tanks for each treatment. The AgNPs stock solution was prepared by dissolving the analytical reagent AgNPs (CAS No. SB25-12DTD; purity ≥ 99.9%; particle size 20 nm; Shanghai Weina Nano Technology Co., China) in sterile seawater.

To evaluate the effects of AgNPs exposure on the physiological functions in *P. tricornutum*, six independent experiments were designed for Microalgae growth inhibition, cellular submicroscopic analysis, apoptosis analysis, mitochondrial membrane potential analysis, and oxidative stress and oxidative damage analysis. In addition, since the N-acetyl-L-cysteine (NAC) was used in the experiments, a solvent experiment was performed to determine that NAC had no significant effect during the experiments. All experiments were performed in triplicate and each sample was measured by triplicate.

2.2.1 Growth inhibition analysis

Triangular brown algae in the exponential growth phase were cultured in f/2 medium with an initial seeding density of 2 × 10^4 cells ml^{-1}, with the total culture volume was 300 ml. Following inoculation, all samples were placed in the same photobioreactor and cultured. Samples were collected at four different time points (24, 48, 72 and 96 h), and 1 mL of culture was extracted at each time point for analysis. Cell counts were performed using a hemocytometer under an optical microscope, the algal cell density was calculated following the method described by Deng (Deng et al., 2017).

2.2.2 Microstructural analysis

Microalgae were exposed to AgNPs with concentrations of 0, 0.01, 2 and 4 mg L^{-1} for 96 h to observe the cell microstructure. After filtering through a membrane, the cells were washed and subjected to low-speed centrifugation at 2000 rpm for 5 min. The collected cells were mixed with a 4% formaldehyde solution diluted in PBS and stored in a refrigerator at 4°C. The cells underwent dehydration using ethanol with a 10% increment rate, followed by infiltration, embedding, and curing. The samples were then sectioned and subjected to double staining with 3% uranyl acetate and lead citrate. Use transmission electron microscopy (TEM) and scanning electron microscope (SEM) to observation.

2.2.3 Apoptosis analysis

The cultivation method for *P. tricornutum*, as described in Section 2.2.1. Cell viability is a crucial parameter for assessing the normalcy of cells. To examine the impact of AgNPs on cell apoptosis, cells were stained using the Anexin V-FITC Cell Apoptosis Detection Kit and analyzed with a flow cytometer. In normal cells, phosphatidylserine (PS) is distributed only on the inner side of the lipid bilayer of the cell membrane. During the early stages of apoptosis, membrane PS flips from the inner side to the outer side of the lipid bilayer. Annexin V, a phospholipid-binding protein, has a high affinity for phosphatidylserine and binds to the cell membrane of early

apoptotic cells by interacting with the externally exposed PS. Therefore, Annexin V serves as a sensitive marker for detecting early apoptosis in cells. Caspase-9 plays a role in the regulation and signal transduction processes of apoptosis. Upon activation, regulatory caspase-9 can catalyze the activation of executioner caspase-3, thereby initiating the cascade reaction of apoptosis. To detect cell apoptosis and measure Caspase-3 and Caspase-9 enzyme activity, the Anexin V-FICT Cell Apoptosis Detection Kit, Caspase-3 Fluorometric Assay Kit, and Caspase-9 Fluorescent Assay Kit from Nanjing Jiancheng Bioengineering Research Institute were used.

2.2.4 Measurement of mitochondrial membrane potential (Δψm)

MMP is one of the important indexes reflecting the normal function of mitochondria. Loss of Δψm may occur in the early stages of apoptosis. Therefore, after exposure to AgNPs for 96 h, samples from all experimental groups were collected, stained with live cells, then MMP was evaluated using flow cytometry (BeamCyte-1026M) to make a measurement, MMP was evaluated with reference to JC-1 mitochondrial membrane potential assay kit (Beyotime Biotechnology) for all parameters, and the changes in cell fluorescence were observed.

2.2.5 Determination of changes in ROS levels and malondialdehyde content

Following the cultivation procedure described in Section 2.2.1, samples were taken at 24, 48, 72, and 96 h, maintaining an algal cell concentration of 3×10^7 cells mL^{-1}. Samples were collected by centrifugation (6000 rpm, 15 min), followed by three washes with phosphate-buffered saline (PBS 0.1 mol/L, pH = 7.2, 4°C). Cell pellets were collected and reserved for further use. ROS was detected using live cells. In the presence of ROS inside the cell, the green fluorescent compound DCF is measured using flow cytometry, indicating the level of ROS. Before measuring Malondialdehyde (MDA), the cells were disrupted using an ultrasonic disruptor (With 3s of disruption followed by 2s of rest, for a total working time of 5 min.). The cell homogenate was centrifuged (6000 rpm, 5 min, 4°C), and the supernatant was collected. The above operations are carried out in accordance with the kit instructions purchased by Nanjing Jiancheng Bioengineering Institute.

2.2.6 Determination of antioxidant enzyme activity and antioxidants

The sample was prepared as in 2.2.5, and the supernatant was taken for determination according to the kit purchased Superoxide dismutase (SOD), Catalase (CAT), Peroxidase (POD), Glutathione peroxidase (GPx), Glutathione reductase (GR) and Glutathione (GSH) by Nanjing Jiancheng Biological Company.

2.2.7 Experiment with the addition of the reactive oxygen species inhibitor N-acetyl-L-cysteine

NAC (powder, purity ≥ 99%) was purchased from Sigma-Aldrich. Prior to use, the concentration of NAC was determined through preliminary experiments to be 300 μM, and NAC stock solution was prepared accordingly. It was ensured that NAC had no significant impact on algal cell growth. The experimental groups included a blank control group, an NAC group, an AgNPs group, and an NAC+AgNPs group. The experimental and control groups were pretreated with 300 μM NAC for 30 min. Subsequently, the corresponding concentrations of AgNPs were added for cell counting experiments. Simultaneously, at 96 h of AgNPs exposure, measurements of ROS levels and cell apoptosis were conducted following the methods outlined in Sections 2.5 and 2.6. Throughout the experimental procedure, stringent aseptic techniques were maintained to ensure the experiments remained free from contamination.

2.3 Data analysis

All data were expressed as the mean ± standard deviation (SD). Prior to running ANOVA, the normality and homogeneity of variance in the data were tested using the Kolmogorov–Smirnov and Levene's tests, respectively. The data met both assumptions and were analysed by ANOVA to examine whether there is significance between groups. If significance was detected, *post hoc* multiple comparisons for between-group differences (LSD multiple comparison) were conducted. Differences were considered significant at $P < 0.05$, $P<0.01$ was considered to have a very significant difference. Data analyses and Graphs were conducted using SPSS 24.0 and Origin 2021.

3 Result

3.1 Microstructural Changes in *P. tricrnutum* Cells Induced by AgNPs Exposure

With the increase in AgNPs concentration, a significant inhibition ($P<0.05$) of *P. tricrnutum* population growth was observed, showing a concentration-dependent effect (Table 1). The control group of *P. tricrnutum* cells exhibits a complete tri-radiate form, with well-defined internal organelles and distinct boundaries (Figure 1). The chloroplast lamellae were closely packed and clear, and the mitochondria cristae were intact and clear.

In comparison to the control group, various degrees of morphological changes were observed in *P. tricrnutum* cells under AgNPs stress (Figure 1). At 0.01 mg L^{-1} stress, there was no significant structural difference in cells compared to the control group. In the 2 mg L^{-1} group, vacuolization of cells intensifies, mitochondria show signs of rupture, and chloroplast membranes exhibit damage, with a looser arrangement of lamellae and some layers appearing fractured. The cell membrane boundary becomes fuzzy, indicating an imminent dissolution of the overall cell structure. In the 4 mg L^{-1} group, chloroplast damage is significant, with loose lamellar structures, chloroplast membranes dissolving, and extensive dissolution of mitochondria. Additionally, the elevated concentration of AgNPs resulted in a significant augmentation in the cellular count of mitochondria, enabling the cell to effectively meet its heightened energy requirements.

Observation from the scanning electron microscopy images (Figure 2), the control group cells were plump, with intact cell

10.3389/fmars.2024.1499109

TABLE 1 Effective concentration (EC_{10}, EC_{20}, EC_{50} and EC_{90}) of AgNPs for *P. tricornutum* growth inhibition at different cultivation times.

Time (h)	Value of EC_X (mg L^{-1})				Regression equation	R^2
	EC_{10}	EC_{20}	EC_{50}	EC_{90}		
24	0.752	1.338	4.025	21.527	y=1.73x-1.04	0.947
48	0.902	1.383	3.133	10.881	y=2.38x-1.18	0.990
72	0.580	0.885	1.984	6.783	y=2.33x-0.67	0.976
96	0.553	0.831	1.817	5.979	y=2.39x-0.59	0.978

membranes and no external attachments. In the stress groups compared to the control group,0.01 mg L^{-1} had the number of mitochondria increased, other than the control group did not change significantly. 2 and 4 mg L^{-1} had cells exhibit noticeable shrinkage, cell walls collapse, some rupture, and cell contents leak out, with the accumulation of AgNPs on the cell walls. This indicates severe internal damage in *P. tricrnutum* under AgNPs stress, with compromised functionality of various organelles.

3.2 Impact of AgNPs exposure on apoptosis, Caspase-3 and Caspase-9 activity in *P. tricrnutum*

The apoptosis rate was determined by the combined proportion of early apoptosis (lower right quadrant) and late apoptosis (upper right quadrant) cells. AgNPs induced apoptosis in *P. tricrnutum* cells in a dose-dependent manner (Figures 3A, B). In the 0.01 mg L^{-1} and 1 mg L^{-1} groups, the number of apoptotic cells slightly increased with AgNPs concentration compared to the control group, with apoptosis rates increasing by 203.6% and 214.4%, respectively. In the 2 mg L^{-1} and 4 mg L^{-1} groups, a significant increase in apoptotic cells was observed, with a respective rise of 337% and 556% ($P < 0.05$). Approximately half of the cells in the 4 mg L^{-1} group were in the apoptotic phase. These results indicate that AgNPs exposure significantly increases the number of apoptotic cells in *P. tricrnutum*.

At 72 h of exposure, caspase-3 activity showed an initial increase followed by a decrease with rising AgNPs concentration (Figure 3C). Except for the 4 mg L^{-1} group, which did not show a significant increase compared to the control group, the other three groups exhibited a significant increase in caspase-3 and Caspase-9 activity, reaching a peak at 1mg L^{-1}, approximately 4.06 times higher than the control group ($P < 0.05$). At 96 h of exposure, except for the 4 mg L^{-1} group, the caspase-3 activity in the other three groups remained significantly elevated compared to the control group ($P < 0.05$). Caspase-9 activity, however, showed a significant increase only in the 0.01 mg L^{-1} and 1 mg L^{-1} groups, with no significant differences in the other three groups compared to the control group.

3.3 Impact of AgNPs exposure on mitochondrial membrane potential

There was no significant change in the 0.01 mg L^{-1} group compared to the control group (Figure 4). However, in the other groups, with the increase of AgNPs concentration, the percentage of JC-1 monomers significantly increases compared to the control group,

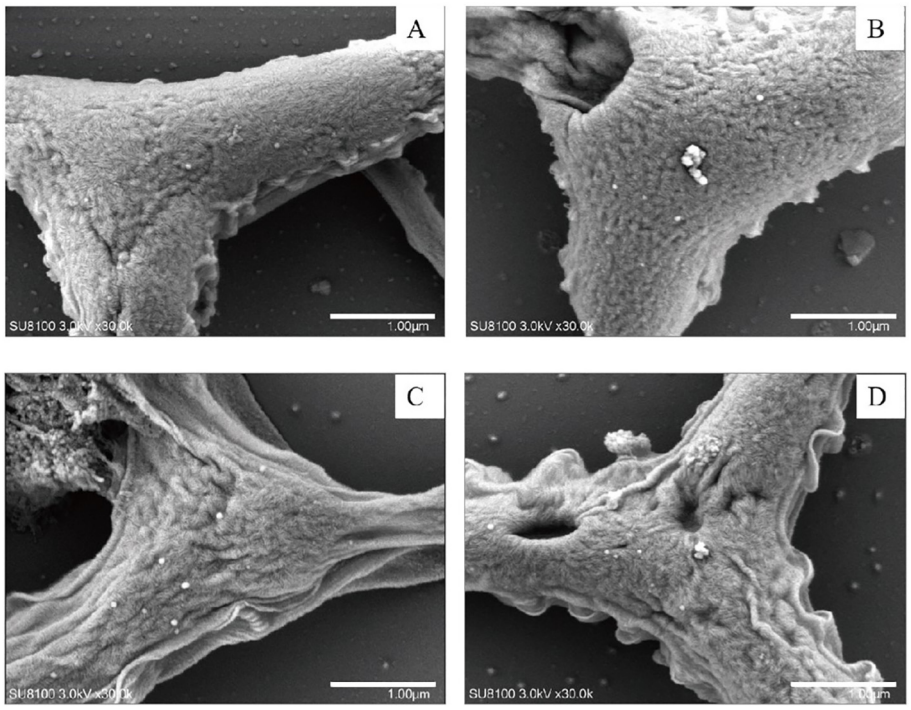

FIGURE 1
Scanning electron microscopy of *P. tricrnutum* cells in the control group **(A)** and AgNPs-exposed after 96 h **(B)** 0.01 mg L^{-1}; **(C)** 2 mg L^{-1}; **(D)** 4 mg L^{-1}.

10.3389/fmars.2024.1499109

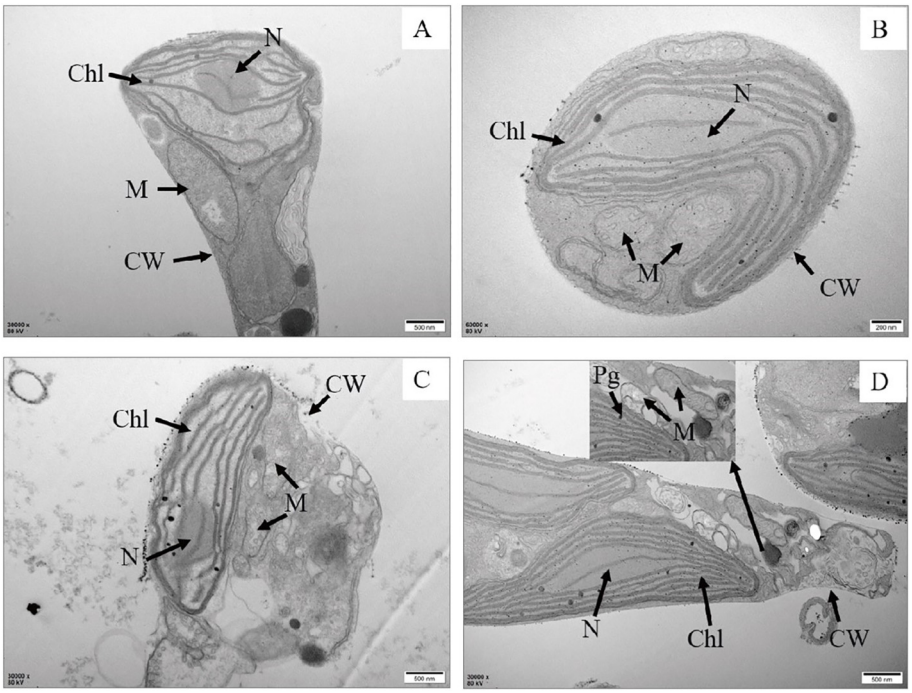

FIGURE 2
Transmission electron microscopy of *P. tricrnutum* cells in the control group **(A)** and AgNPs-exposed after 96 h **(B)** 0.01 mg L^{-1}; **(C)** 2 mg L^{-1}; **(D)** 4 mg L^{-1}) Chl, chloroplast; M, mitochondria; Pg, plastoglobuli; CW, cell wall; N, nucleus.

showing a concentration-dependent relationship. This indicates a decrease in MMP levels and damage to the mitochondrial membrane.

3.4 Impact of AgNPs Exposure on MDA and ROS content in *P. tricornutum*

After 24 h of exposure, the ROS levels increased with the concentration of AgNPs, and except for the 0.01 mg L^{-1} group, all other groups showed a significant rise compared to the control group (Figure 5A), ($P < 0.05$). After 48 h of exposure, there was a significant increase in ROS levels in the stressed groups compared to the control group. After 72 h of exposure, the ROS levels in the 0.01 mg L^{-1} group showed no significant difference from the control group ($P > 0.05$), while all other groups still significantly exceeded the ROS levels of the control group ($P < 0.05$). Overall, exposure to AgNPs resulted in a pronounced rise in ROS and MDA levels within the cells. The experimental results showed that with the increase of AgNPs concentration, ROS levels were significantly higher than those in the control group. After 96 h of exposure, the existing environmental concentration of AgNPs did not notably influence the ROS levels in algal cells.

At 24 h of exposure, MDA content increased with the increase of AgNPs concentration, which was significantly higher than that of the control group ($P < 0.05$) (Figure 5B). When the exposure time exceeded 48h, the MDA content increased first and then decreased, but it was still significantly higher than that of the control group ($P < 0.05$). At 72 h after exposure, MDA content in exposed groups was still higher than that in control group ($P < 0.05$). When the exposure time was 96h, there was no significant difference in MDA content between the 0.01mg L^{-1} group and the control group ($P > 0.05$). In general, with the increase of AgNPs content, MDA content showed an obvious trend of first increasing and then decreasing, and MDA content in the stress group was higher than that in the control group.

3.5 Impact of AgNPs Exposure on Antioxidant Enzyme Content in *P. tricornutum*

During the 24 h exposure, the SOD activity at various concentrations showed no significant changes ($P>0.05$) (Figure 6A). After 48 h of exposure, the SOD activity at 0.01 and 1 mg L^{-1} increased by 37.37% and 83.55% respectively, compared to the control group, while the activity at 4 mg L^{-1} decreased by 23.63%. At 72 h, the SOD activity at 0.01 and 1 mg L^{-1} was significantly higher than that of the control group ($P<0.05$), while the 2 and 4 mg L^{-1} groups were significantly lower ($P<0.05$). After 96 h of exposure, SOD activity at 1, 2 and 4 mg L^{-1} showed a significant decrease compared to the control group ($P<0.05$).

For POD activity, during the 24 h exposure (Figure 6B), there was no significant difference between the 0.01 and 1 mg L^{-1} groups and the control group ($P>0.05$), whereas the 2 and 4 mg L^{-1} groups showed a significant increase ($P<0.05$), rising by 39.40% and 41.03% respectively. After 48 h, the POD activity continued to increase in the 2 and 4 mg L^{-1} groups, with the 1 mg L^{-1} group also showing an

10.3389/fmars.2024.1499109

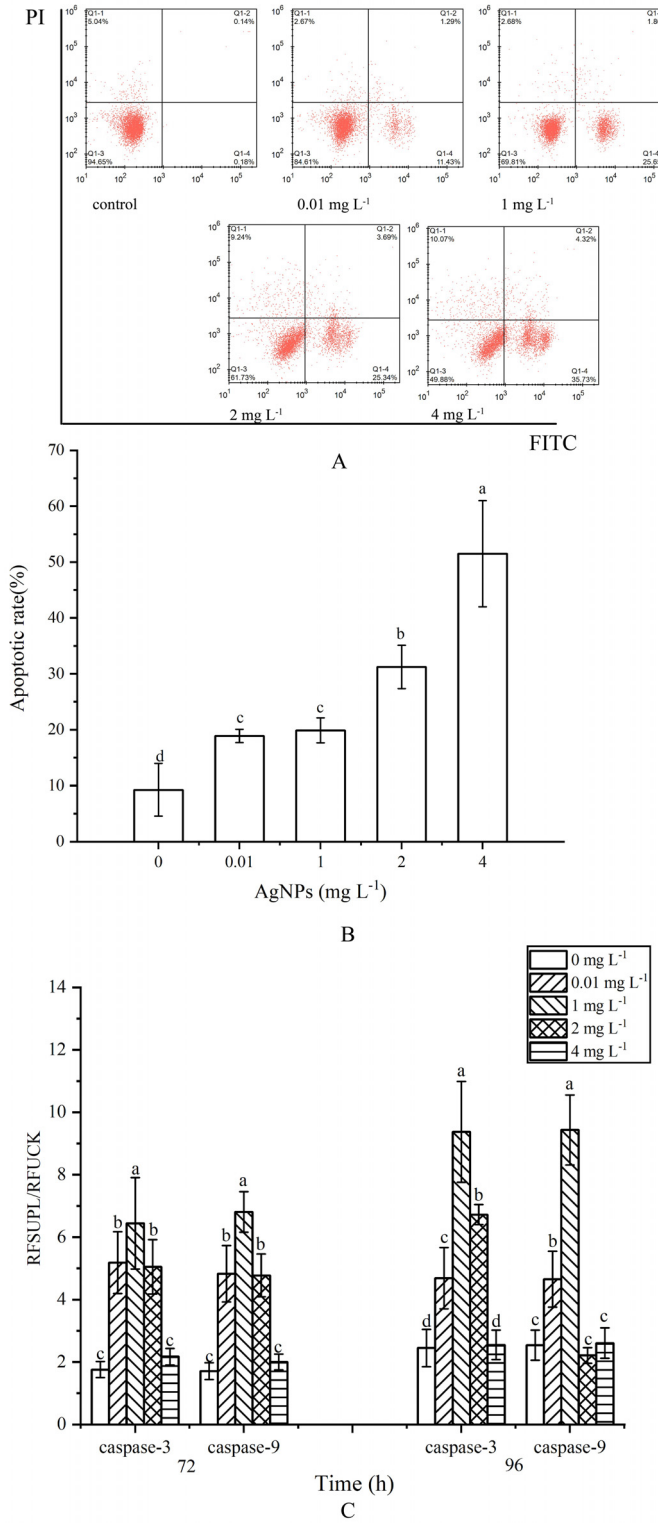

FIGURE 3
Impact of AgNPs Exposure on Apoptosis and Caspase-3, Caspase-9 Activities in *P. tricrnutum* **(A)** Histogram of flow cytometry, **(B)** column diagram of flow analysis, **(C)** caspase activity.

increase, all significantly higher than the control group ($P<0.05$). At 72 h, there were no significant differences between all exposure groups and the control group ($P>0.05$). By 96 h, the POD activity at 1, 2 and 4 mg L^{-1} showed a significant decrease compared to the control group ($P<0.05$), with reductions of 38.26%, 70.81% and 74.81% respectively.

Regarding CAT activity, during the 24 h exposure (Figure 6C), the 1, 2 and 4 mg L^{-1} groups exhibited significant increases compared

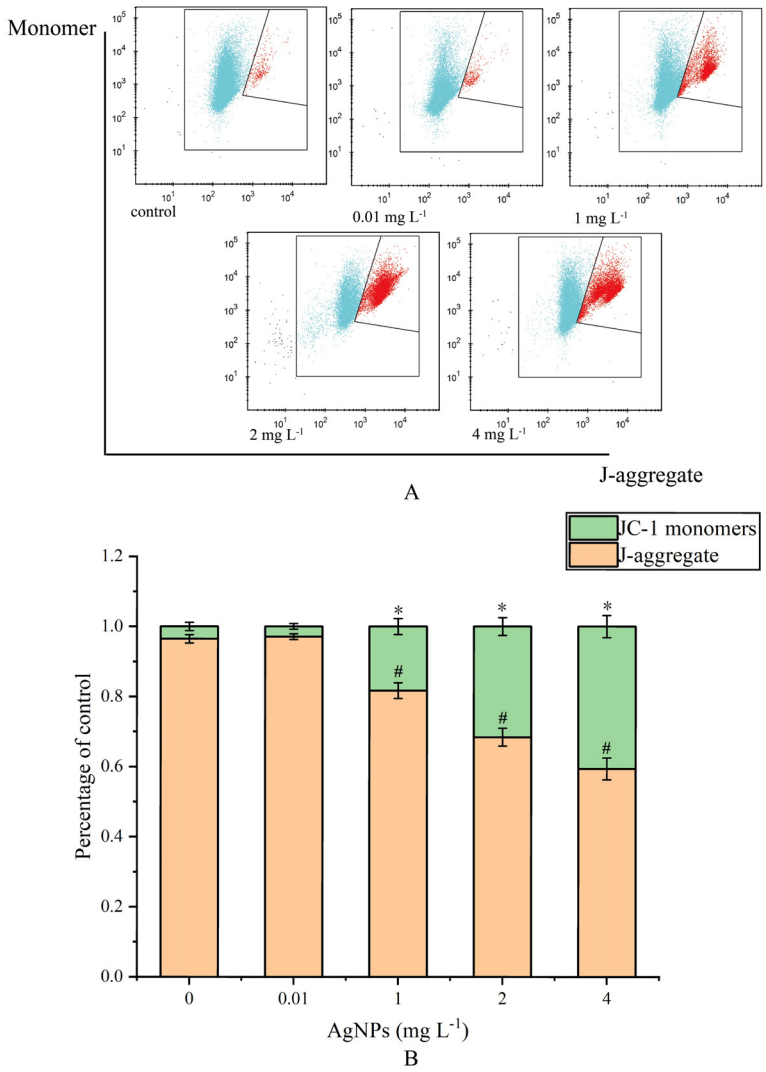

FIGURE 4
Impact of AgNPs Exposure on MMP **(A)** Histogram of flow cytometry, **(B)** column diagram of flow analysis, * means that JC-1 monomers differ significantly from the control group, # means that J-aggregate differs significantly from the control group).

to the control group (P<0.05), with increases of 43.15%, 64.46% and 83.32% respectively. After 48 h, the 1, 2 and 4 mg L^{-1} groups still showed significant increases compared to the control group (P<0.05), with increases of 17.79%, 47.48% and 57.21% respectively. At 72 h, there was no significant difference in CAT activity between the 0.01 and 1 mg L^{-1} groups and the control group (P>0.05), while the 2 and 4 mg L^{-1} groups showed a significant decrease (P<0.05). After 96 h of exposure, the CAT activity at 1, 2 and 4 mg L^{-1} significantly decreased compared to the control group (P<0.05), with reductions of 58.64%, 81.77% and 74.96% respectively.

GSH-Px activity exhibited an initial increase followed by a decrease with the rise in AgNPs concentration and exposure time (Figure 7A). h After 24 h of exposure, GSH-Px activity significantly increased compared to the control group (P < 0.05). At 48 h of exposure, the 1, 2 and 4mg L^{-1} groups showed a significant increase compared to the control group (P < 0.05), while the 0.01 mg L^{-1} groups exhibited no significant difference (P>0.05). At 72 h of exposure, GSH-Px activity showed an increasing trend with AgNPs concentration, with significant increases in the 0.01, 1 and 2 mg L^{-1} groups compared to the control group (P < 0.05). At 96 h of exposure, the 2 and 4 mg L^{-1} groups exhibited a significant decrease compared to the control group (P<0.05), with activity reductions of 23.28% and 33.94% respectively. The 0.01 and 1 mg L^{-1} groups showed no significant change in GSH-Px content compared to the control group (P>0.05).

GR activity exhibited a trend of initial increase followed by a decrease with the rise in AgNPs concentration (Figure 7B). After 24 h of exposure, all stress groups showed a significant increase in GR activity compared to the control group (P < 0.05), reaching a peak at 1 mg L^{-1}. At 48 h of exposure, stress groups still displayed a significant increase in GR activity compared to the control group (P < 0.05). After 72 h of exposure, GR activity increased first and then decreased, and was significantly higher than that of the control group at 0.01,1 and 2 mg L^{-1}(P <0.05); h the 4 mg L^{-1} group showed

10.3389/fmars.2024.1499109

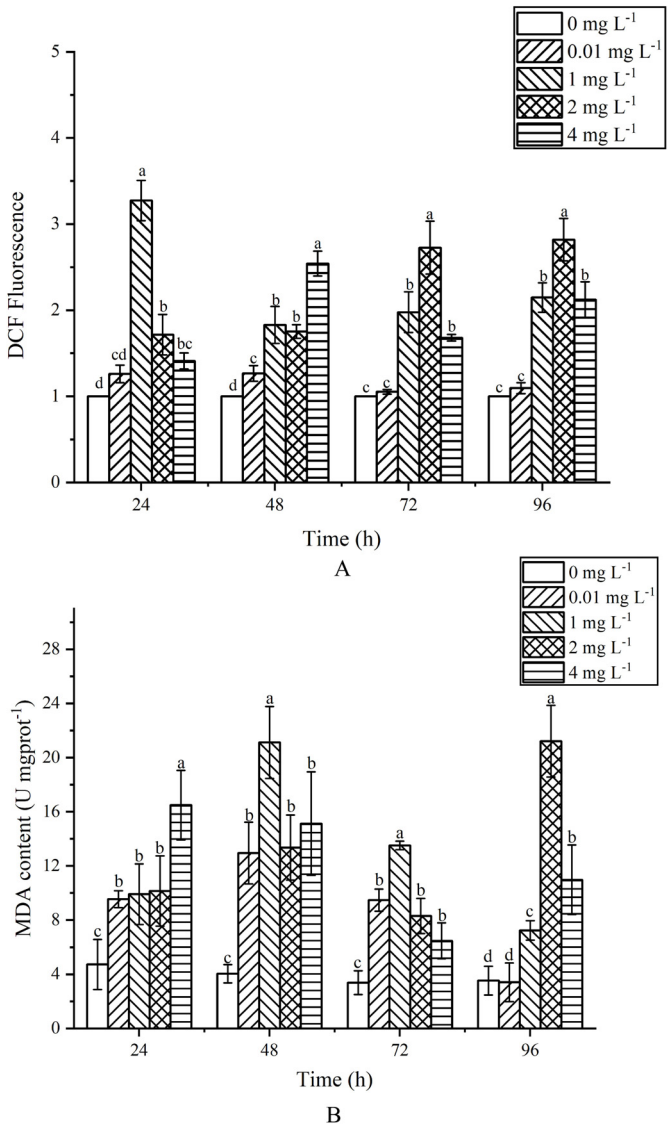

FIGURE 5
Effects of AgNPs exposure at different concentrations on MDA and ROS content in *P. tricornutum* **(A)** column diagram of flow analysis, **(B)** MDA content).

no significant change compared to the control group ($P < 0.05$). At 96 h of exposure, the 0.01, 1 and 2 mg L^{-1} groups showed activity increases of 30.24%, 27.04% and 20.03% ($P < 0.05$) respectively, compared to the control group. The 4 mg L^{-1} group exhibited a significant decrease compared to the control group.

3.6 Impact of AgNPs Exposure on the Antioxidant Substance Content within *P. tricornutum*

The content of GSH in *P. tricornutum* exposed to AgNPs exhibited a trend of initial increase followed by a decrease with increasing exposure time (Figure 8). At 24 h of exposure, the GSH content increased with increasing AgNPs concentration. When the concentration reached 1 mg L^{-1}, there was a significant difference in GSH content compared to the control group ($P < 0.05$). When the concentration reached 2 mg L^{-1}, it peaked, showing a 34.42% increase compared to the control group. In the 4 mg L^{-1} group, there was a significant downward trend compared to the control group ($P < 0.05$), and with increasing exposure time, the GSH content in the 4 mg L^{-1} group showed little change. At 48 h of exposure, the GSH content peaked in the 1 mg L^{-1} group, with a 28.59% increase compared to the control group. Although the GSH content in the 2 mg L^{-1} group decreased compared to 24 h, it still showed a significant increase compared to the control group ($P < 0.05$). With increasing exposure time, the GSH content in the 0.01 mg L^{-1}, 1 mg L^{-1}, and 2 mg L^{-1} groups gradually returned to values similar to the control group. Although the GSH content was slightly higher than that of the control group, there were no significant differences ($P < 0.05$).

10.3389/fmars.2024.1499109

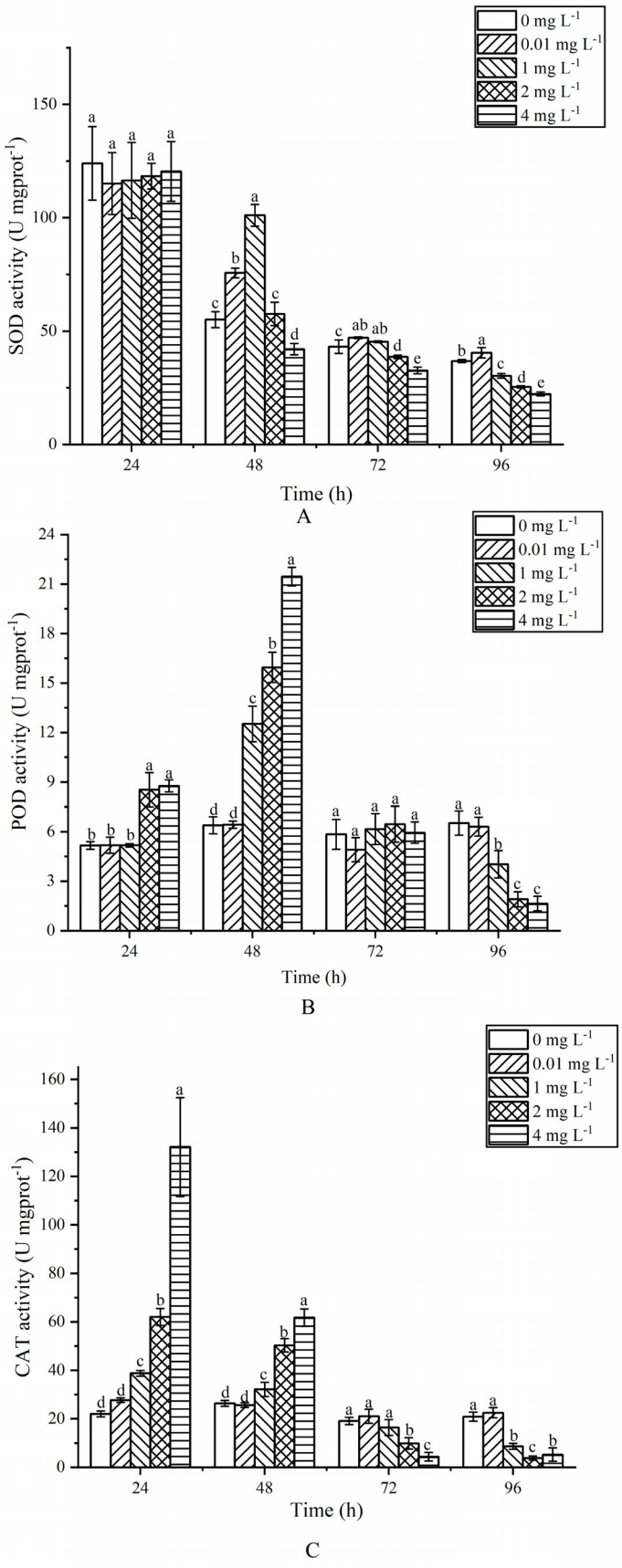

FIGURE 6
Effects of AgNPs exposure at different concentrations on SOD **(A)**, POD **(B)** and CAT **(C)** activity of *P. tricornutum*.

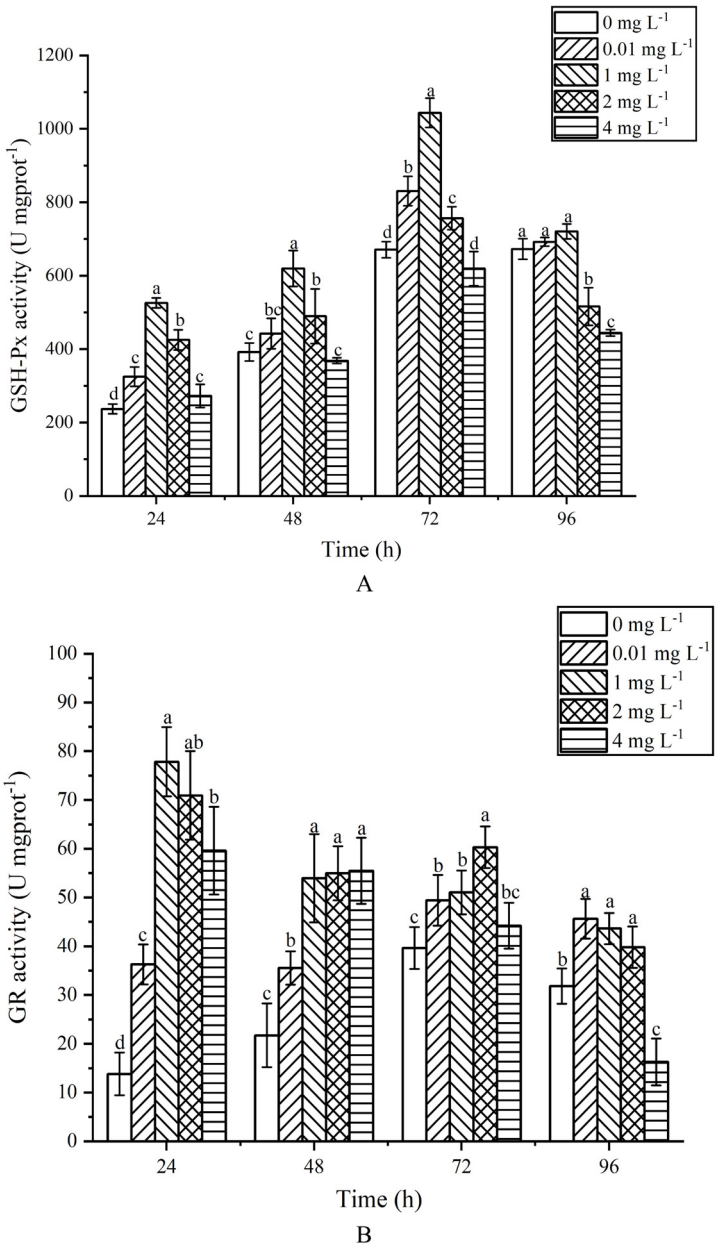

FIGURE 7
Effects of AgNPs exposure at different concentrations on GSH-Px **(A)** and GR **(B)** activity of *P. tricornutum*.

3.7 Impact of NAC on the Growth, ROS Levels, and Apoptosis of *P. tricrnutum* Under AgNPs Exposure

The influence of the addition of NAC on cell growth was shown (Figure 9A). Compared to the control group, the addition of 300 μM NAC did not significantly affect algal growth, indicating its suitability as an experimental additive. After the addition of AgNPs, the cell count in the 0.01 mg L^{-1} group showed no significant change compared to the control group, while the cell count in the other three groups decreased with increasing AgNPs concentration. Simultaneously, the addition of AgNPs and NAC resulted in a significant increase in cell count in all groups, with no significant change compared to the control group.

The variation in ROS levels after the addition of NAC was depicted (Figures 9B, C). Adding only NAC showed no significant change in ROS levels compared to the control group. However, in the 2 mg L^{-1} AgNPs group, the addition of NAC led to a significant reduction in ROS levels, approximately a 41.5% decrease. Moreover, the addition of NAC effectively inhibited cell apoptosis (Figure 10), with the proportion of cells in the apoptotic phase showing no significant difference compared to the control group in all stress groups. Therefore, the addition of NAC can effectively suppress ROS production and reduce AgNPs-induced cell apoptosis.

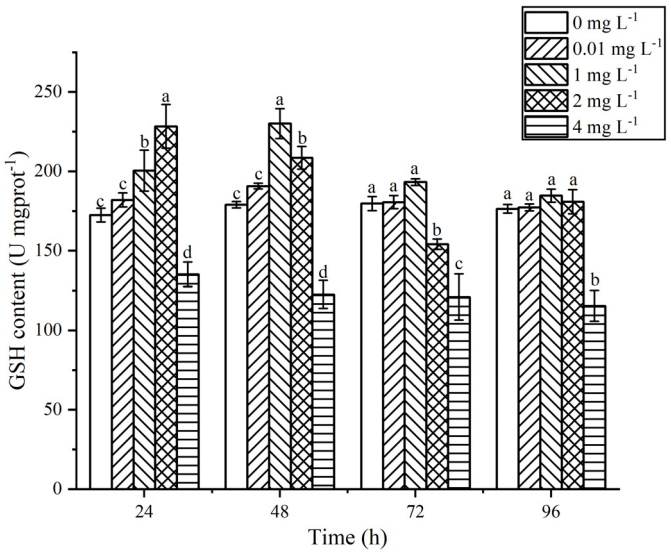

FIGURE 8
Effects of AgNPs exposure at different concentrations on GSH content in *P. tricornutum*.

4 Discussion

AgNPs is widely used because of its characteristics, and it will cause harm to Marine organisms when it gathers into the ocean in various ways. Current studies have shown that AgNPs can cause cell apoptosis in aquatic animals, and at the same time, it can destroy cell structure and cause cells to be unable to perform normal physiological activities. However, there is no systematic study on the toxin production mechanism and toxic effects of AgNPs causing cell apoptosis. Therefore, in this paper, the damage of AgNPs to Marine algae was investigated by measuring the changes of apoptosis and antioxidant system of *P.tricornutum* after AgNPs stress.

TEM and SEM results showed that AgNPs particles were attached outside the cell, cell surface was crumped, cell membrane was broken, organelles were damaged, and chloroplasts and mitochondria were seriously damaged. This will lead to insufficient energy supply of the cell itself and changes in the cellular environment, which may result in a series of reactions such as oxidative stress (Gurgueira and Franco, 2011). To this end, we examined the substances produced by cellular mitochondria and cellular oxidative stress.

Apoptosis refers to the process of gene-controlled, orderly, autonomous cell death that maintains homeostasis (Lugovaya et al., 2020). When apoptosis occurs, a large amount of PS is externalized on the cell membrane surface, serving as an "eat me" signal released by apoptotic cells, thereby mediating apoptosis (Meehan et al., 2016). The number of PS-externalized cells is considered a marker for monitoring phytoplankton cell apoptosis. In this study, flow cytometry and morphological changes showed that apoptosis occurred within a short period, and the number of PS-externalized cells increased with higher concentrations of AgNPs (Figure 3). Meanwhile, the proportion of non-apoptotic cells gradually decreased, indicating that AgNPs induced apoptosis in *P.tricornutum*. Mitochondrial-mediated apoptosis is a crucial pathway for cell apoptosis. In the early stages of apoptosis, the mitochondrial structure is disrupted, membrane permeability increases, and the MMP declines or even disappears. The decrease in MMP is considered one of the earliest biological changes during apoptosis. In this study, AgNPs significantly reduced the MMP of *P.tricornutum* (Figure 4) and caused morphological changes such as lighter mitochondrial matrix, shorter and fewer cristae, and vacuolization of mitochondria (Figure 1). This is similar to the mitochondrial damage observed in *Chlorella vulgaris* exposed to AgNPs (Barreto et al., 2019). Moreover, studies have shown that exposure to pollutants can stimulate the activity of caspase family enzymes, thereby inducing apoptosis. Caspase-9 plays a role in regulating and signaling apoptosis; once activated, it can catalyze the activation of executioner caspase-3, initiating the apoptotic cascade. This study found that AgNPs stress increased the activity of caspase-3 and caspase-9, indicating that AgNPs can enhance the activity of these enzymes to trigger programmed cell death. Therefore, AgNPs may initiate mitochondrial-mediated apoptosis by disrupting mitochondrial structure, decreasing MMP, and increasing the activity of caspase family enzymes in *P.tricornutum*.

ROS are widely present in organisms and are by-products of normal oxygen metabolism. They participate in normal material circulation and signal transduction within the body. When cells are subjected to harmful external factors, a large amount of ROS can be produced, which can damage cell membranes, DNA, and protein structures, leading to the loss of cellular homeostasis. The results of this study also indicate that exposure to AgNPs leads to a significant

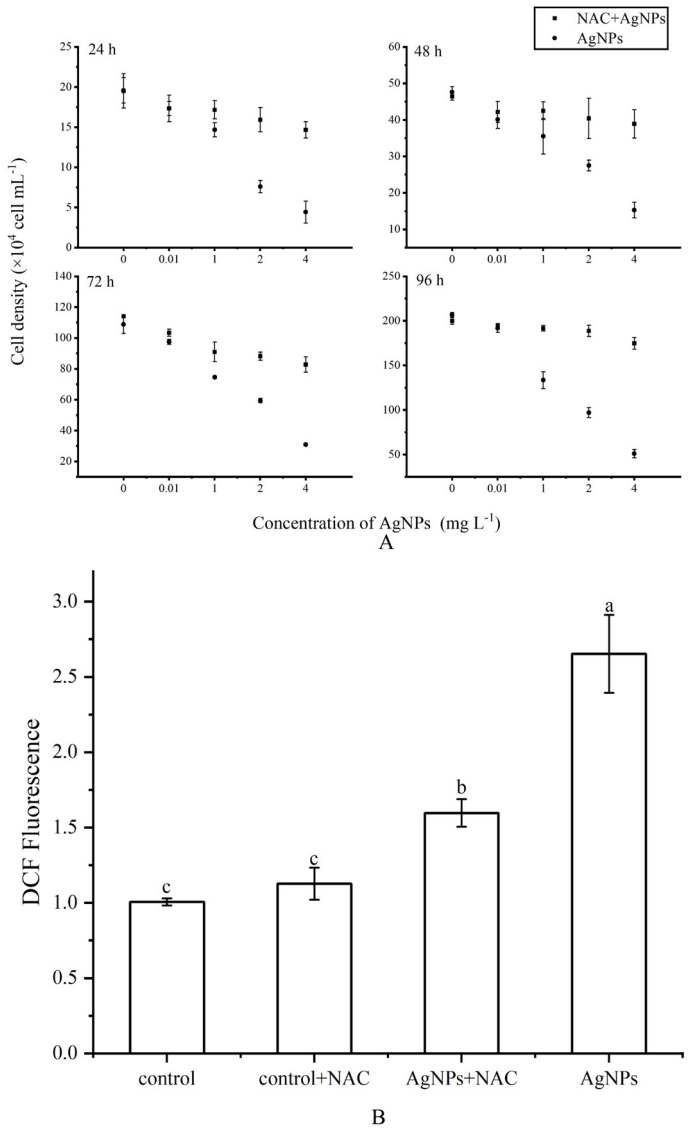

FIGURE 9
Effect of NAC on ROS levels of *P. tricornutum* under AgNPs **(A)** growth inhibition **(B)** column diagram of flow analysis AgNPs concentration: 2 mg L^{-1}).

increase in ROS levels within algal cells, demonstrating that *P.tricornutum* experiences oxidative stress under AgNPs stress.

Excess ROS cancause lipid peroxidation, leading to the production of MDA (Liu et al., 2019). High levels of MDA can aggregate with macromolecules such as proteins within cells, thereby disrupting cell membrane structure (Huang et al., 2020), leading to organelle damage.In this experiment, as the concentration of AgNPs exposure increased, the MDA content significantly increased, indicating that AgNPs induce an increase in ROS levels, causing lipid peroxidation in *P.tricornutum* and thereby damaging algal cells. Cell electron microscopy analysis showed that under 2 mg L^{-1} AgNPs exposure, mitochondrial damage prevented normal respiration. Mitochondria are also a primary source of oxidative stress, generating substantial amounts of ROS during oxidative phosphorylation. The increase in ROS levels triggers an antioxidant response within the organism, aiming to mitigate the damage caused by ROS (Chaufan et al., 2006). In algal cells, SOD, CAT, and POD represent the first line of defense against oxidative stress. These enzymes are typically considered among the most direct biological indicators of oxidative stress. When algal cells are subjected to stress, they can mitigate the damage caused by ROS, thereby maintaining cellular stability. In this experiment, when *P. tricornutum* was exposed to AgNPs, the activities of SOD, CAT, and POD significantly increased to eliminate excess ROS and prevent membrane lipid peroxidation.

GSH-Px and GR belong to the phase II detoxification enzyme family (Li et al., 2023). GSH-Px is widely present in organisms and prevents protein hydrolysis by combining with GSH to remove excess ROS from the body (Penninckx and Jaspers, 1993). Under AgNPs stress, GSH-Px activity is enhanced, promoting the binding of GSH to

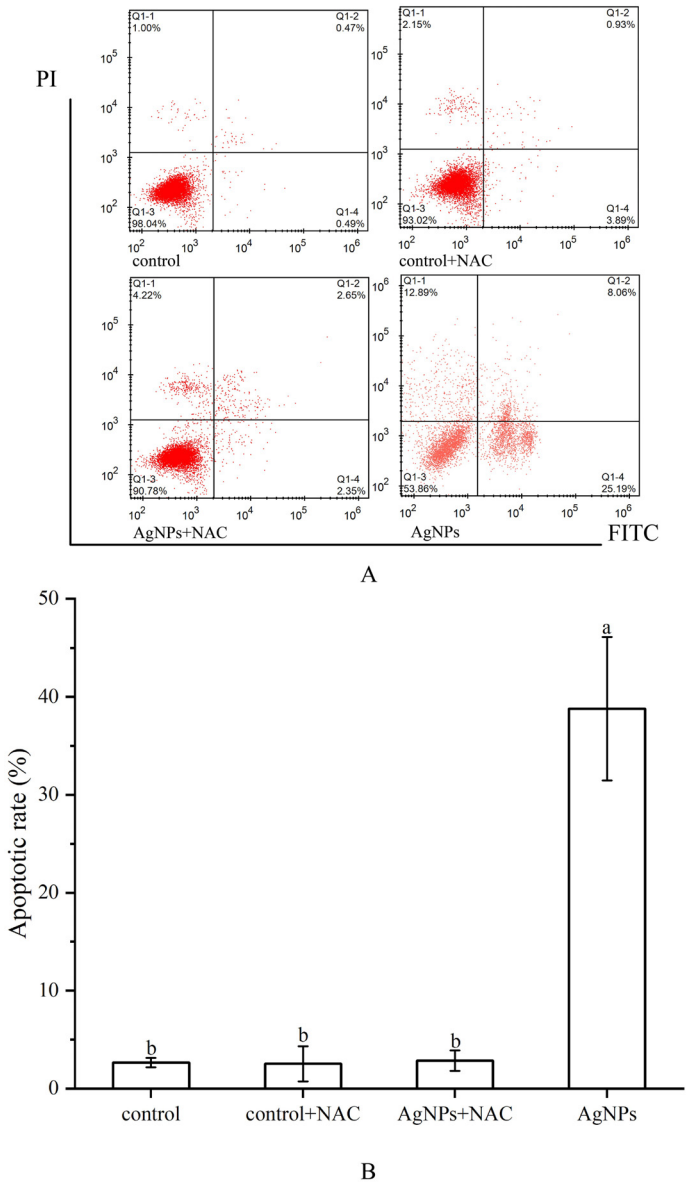

FIGURE 10
Effect of NAC on apoptosis of *P. tricornutum* cells treated by AgNPs (AgNPs concentration: 2 mg L^{-1} **(A)** Histogram of flow cytometry, **(B)** column diagram of flow analysis).

ROS and thereby reducing ROS-induced cellular damage. Concurrently, the substantial consumption of GSH stimulates GR activity to reduce oxidized glutathione (GSSH) back to GSH (Mufeed et al., 2018), maintaining intracellular antioxidant stability and preventing excess ROS-induced damage. In this experiment, as the concentration of AgNPs increased, the activities of GSH-Px and GR also increased to counteract the oxidative damage caused by ROS to *P.tricornutum*. However, with prolonged exposure to AgNPs, the activities of SOD, CAT, POD, GSH-Px, and GR showed a significant decline compared to the control group, exhibiting a trend of initial increase followed by a decrease over time. This phenomenon may be attributed to significant damage to various cellular organelles over time, resulting in reduced antioxidant enzyme production. Additionally, damage to mitochondria and chloroplasts could impair the cell's ability to generate sufficient energy to combat oxidative stress, further diminishing antioxidant enzyme activity. Similar trends have been observed in studies on the *Halamphora veneta* and *Surirella crumena* (Jia, 2019), where the activities of

TABLE 2 Pearson's correlation coefficients of some test indicators of *P. tricornutum* cells under AgNPs stress (96 h).

	IR(%)	ROS	JC-1 monomers	J-aggregates
ROS	0.847**			
JC-1 monomers	0.983**	0.924**		
J-aggregates	-0.983**	-0.924**	-1.000**	
Apoptotic rate	0.897**	0.947**	-0.929**	0.931**

**Significant differences at the $P < 0.01$ level.

antioxidant enzymes initially increased and then decreased with rising concentrations of cadmium and lead.

Previous studies have suggested that pollutants can induce the accumulation of ROS in microalgal cells, with the resulting oxidative damage potentially serving as a mechanism of toxicity to aquatic organisms exposed to these pollutants (Lobato et al., 2023). In this study, Pearson correlation analysis (Table 2) revealed a positive correlation between ROS levels and both growth inhibition rate ($r = 0.847$) and apoptosis rate ($r = 0.897$), suggesting that increased oxidative stress is associated with enhanced growth inhibition and cell apoptosis. Furthermore, pretreatment with the ROS inhibitor NAC can attenuate AgNPs-induced cell apoptosis and growth inhibition. Therefore, excessive production of ROS may be involved in AgNPs-induced cell apoptosis and AgNPs-mediated growth inhibition. Regarding how excessive ROS mediates the toxicity of AgNPs in *P. tricrnutum*, we speculate that its mechanism is related to mitochondria, which are the main source of ROS in cells and also the target of ROS. Indeed, accumulation of excessive ROS may lead to increased permeability of the mitochondrial membrane, resulting in a decrease or even disappearance of MMP, ultimately leading to cell apoptosis. TEM images obtained in this study showed that in the high AgNPs concentration group, the mitochondria of algal cells were significantly disintegrated (severely vacuolated), with the internal structure tending to be simple, indicating that they were on the verge of disintegration. These morphological features are consistent with the reported expression of apoptotic morphological markers in single-cell photosynthetic plants by Kasuba et al (Mohammadi et al., 2021; Lin et al., 2023). Under ROS-mediated stress conditions, the observed organelle-specific oxidative stress pattern and antioxidant capacity appear to modulate cell apoptosis. Therefore, we propose a positive feedback loop of apoptosis signaling: AgNPs stress causes the generation of ROS in mitochondria and the enhancement of the activity of intracellular antioxidant enzymes. With the accumulation of ROS, the mitochondrial membrane is further damaged to accelerate the generation of apoptosis, and at the same time, the activity of intracellular antioxidant enzymes is decreased.

In conclusion, this study found that AgNPs exhibit an inhibitory effect on the growth of *P. tricornutum*, induce changes in cell morphology, and trigger oxidative stress responses in a concentration-dependent manner. The experimental data demonstrated that exposure to AgNPs generates ROS, leading to lipid peroxidation and membrane damage, which disrupts membrane integrity and causes changes in mitochondrial membrane potential (MMP). These effects ultimately alter the physiological and biochemical functions of the cells, resulting in apoptosis. The findings of this study contribute to a better understanding of the ecological risks posed by AgNPs released into aquatic environments and provide valuable data for assessing their impact on the marine ecosystem.

Data availability statement

The original contributions presented in the study are included in the article/supplementary material. Further inquiries can be directed to the corresponding author.

Author contributions

YZ: Writing – original draft, Conceptualization, Methodology, Software. CL: Writing – review & editing, Methodology, Software. BL: Writing – review & editing, Methodology. LC: Writing – review & editing, Data curation. ZX: Validation, Writing – review & editing. XT: Supervision, Writing – review & editing. CS: Writing – review & editing, Methodology. JG: Writing – review & editing, Supervision. RQ: Writing – review & editing, Investigation. SH: Data curation, Funding acquisition, Resources, Supervision, Writing – review & editing.

Funding

The author(s) declare financial support was received for the research, authorship, and/or publication of this article. This work was financially supported by the National Youth Natural Science Foundation of China (42106154), Natural Science Foundation of Shandong Province (ZR2019BD011).

Acknowledgments

The authors thank all the laboratory staff.

Conflict of interest

The authors declare that the research was conducted in the absence of any commercial or financial relationships that could be construed as a potential conflict of interest.

Publisher's note

References

Atta, A. H., El-Ghamry, M. A., Hamzaoui, A., and Refat, M. S. (2015). Synthesis and spectroscopic investigations of iron oxide nano-particles for biomedical applications in the treatment of cancer cells. *J. Mol. Structure* 1086, 246–254. doi: 10.1016/j.molstruc.2014.12.085

Barreto, D. M., Tonietto, A. E., Amaral, C. D. B., Pulgrossi, R. C., Polpo, A., Nóbrega, J. A., et al. (2019). Physiological responses of *Chlorella sorokiniana* to copper nanoparticles. *Environ. Toxicol. Chem.* 38, 4332. doi: 10.1002/etc.v38.2

Campbell, L. A., Gormley, P. T., Bennett, J. C., Murimboh, J. D., and MacCormack, T. J. (2019). Functionalized silver nanoparticles depress aerobic metabolism in the absence of overt toxicity in brackish water killifish, Fundulus heteroclitus. *Aquat. Toxicol.* 213, 105221. doi: 10.1016/j.aquatox.2019.105221

Châtel, A., Lièvre, C., Barrick, A., Bruneau, M., and Mouneyrac, C. (2018). Transcriptomic approach: A promising tool for rapid screening nanomaterial-mediated toxicity in the marine bivalve Mytilus edulis—Application to copper oxide nanoparticles. *Comp. Biochem. Physiol. Part C: Toxicol. Pharmacol.* 205, 26–33. doi: 10.1016/j.cbpc.2018.01.003

Chaufan, G., Juárez, A., Basack, S., Ithuralde, E., Sabatini, S. E., Genovese, G., et al. (2006). Toxicity of hexachlorobenzene and its transference from microalgae (*Chlorella kessleri*) to crabs (*Chasmagnathus granulatus*). *Toxicology* 227, 3, 262–270. doi: 10.1016/j.tox.2006.08.011

Chen, C. P., Gao, Y. H., and Lin, P. (2006). Production of extracellular polymeric substances (EPS)by benthic diatom: effect of salinity and pH. *Haiyang Xuebao* 28, 123–129.

Chinnapongse, S. L., Maccuspie, R. I., and Hackley, V. A. (2011). Persistence of singly dispersed silver nanoparticles in natural freshwaters, synthetic seawater, and simulated estuarine waters. *Sci. total Environ.* 409, 2443–2450. doi: 10.1016/j.scitotenv.2011.03.020

Cui, L., Xu, W., Guo, X., Zhang, K., Wei, Q., and Du, D. (2014). Synthesis of strontium hydroxyapatite embedding ferroferric oxide nano-composite and its application in Pb^{2+} adsorption. *J. Mol. Liquids* 197, 40–47. doi: 10.1016/j.molliq.2014.04.027

Dash, A., Singh, A. P., Chaudhary, B. R., Singh, S. K., and Dash, D. (2012). Effect of silver nanoparticles on growth of eukaryotic green algae. *Nano-Micro Lett.* 4, 158–165. doi: 10.1007/BF03353707

Deng, X. Y., Li, D., Wang, L., Hu, X. L., Cheng, J., and Gao, K. (2017). Potential toxicity of ionic liquid ([C12mim]BF4) on the growth and biochemical characteristics of a marine diatom *Phaeodactylum tricornutum*. *Sci. Total Environ.* 586, 675–684. doi: 10.1016/j.scitotenv.2017.02.043

Elsheekh, M. M., and Elkassas, H. Y. (2014). Application of biosynthesized silver nanoparticles against a cancer promoter cyanobacterium, microcystis aeruginosa. *Asian Pacific J. Cancer Prev. Apjcp* 15, 6773–6779. doi: 10.7314/APJCP.2014.15.16.6773

Gurgueira, S. A., and Franco, A. (2011). Effect of acetylsalicylic acid on mitochondrial function and antioxidant enzyme activities in cho cells. *Free Radical Biol. Med.* 51, 87. doi: 10.1016/j.freeradbiomed.2011.10.402

Hassanpour, M., Tafreshi, A. H., Amiri, O., Hamadanian, M., and Niasari, M. S. (2021). Toxicity of Nd_2WO_6 nanoparticles to the microalga Dunaliella salina: synthesis of nanoparticles and investigation of their impact on microalgae. *RSC Adv.* 11, 27283–27291. doi: 10.1039/D1RA04878C

Hong, B., Jiang, L., Xue, H., Liu, F. Y., Jia, M., Li, J., et al. (2014). Characterization of nano-lead-doped active carbon and its application in lead-acid battery. *J. Power sources* 270, 332–341. doi: 10.1016/j.jpowsour.2014.07.145

Huang, G. Q., Yu, X., and Lu, Q. Q. (2023). Research on spatial interpolationmethod of regional VOCs massconcentration based on BOA-ELM. *J. Saf. Environ.* 09), 3371–3377.

Huang, M., Keller, A. A., Wang, X., Tian, L. Y., Wu, B., Ji, R., et al. (2020). Low concentrations of silver nanoparticles and silver ions perturb the antioxidant defense system and nitrogen metabolism in N2-fixing cyanobacteria. *Environ. Sci. Technol.* 54, 15996–16005. doi: 10.1021/acs.est.0c05300

Jia, K. (2019). Toxicological effects of heavy metal cadmium Cd^{2+} and lead Pb^{2+} stress on two diatoms. Harbin Normal University, Harbin.

Johnson, M. S., Songkiatisak, P., Cherukuri, P. K., and Xu, X. H. N. (2022). Toxic effects of silver ions on early developing zebrafish embryos distinguished from silver nanoparticles. *ACS Omega* 7, 40446–40455. doi: 10.1021/acsomega.2c05504

Jun, H. (2016). Environmental toxicology and toxicitymechanism of silver nanoparticles onmarine microalgae. (Shanghai, China: East China Normal University).

Li, M. G., Zhang, Y. Y., Qiao, X. L., and Song, D. Y. (2023). Function of the glutathione peroxidase family and the potential of its members as markers of immunotherapy in glioma. *Chin. J. Cancer Biotherapy* 30, 997–1008.

Lin, W., Wu, J., Luo, H., Liu, X. L., Cao, B. B., Hu, F., et al. (2023). Sub-chronic ammonia exposure induces hepatopancreatic damage, oxidative stress, and immune dysfunction in red swamp crayfish (*Procambarus clarkii*). *Ecotoxicology Environ. Saf.* 254, 114724. doi: 10.1016/j.ecoenv.2023.114724

Liu, Y. F., Wang, W. W., Zu, Y. X., Mei, Y., Zheng, J. Q., Wu, Y. C., et al. (2019). Research progress on the effects of catalase on plant stress tolerance. *Barley Cereal Sci.* 36, 5–8.

Lobato, M. C., Feldman, M. L., MaChinandiarena, M. F., and Olivieri, F. P. (2023). First insights into the role of polyamines in biotic stress resistance induced by potassium phosphite in potato. *Potato Res.* 67, 255–270. doi: 10.1007/s11540-023-09633-9

Lugovaya, A. V., Kalinina, N. M., Mitreikin, V. P., Emanuel, Y. V., Kovalchuk, Y. P., and Artyomova, A. V. (2020). Spontaneous and activation-induced apoptosis of peripheral blood mononuclear cells in the pathogenesis of type 1 diabetes mellitus. *Med. Immunol. (Russia)* 22, 1834. doi: 10.15789/1563-0625-saa-1834

Mansour, W., Abdelsalam, N. R., Tanekhy, M., Khaled, A. A., and Mansour, A. T. (2021). Toxicity, inflammatory and antioxidant genes expression, and physiological changes of green synthesis silver nanoparticles on Nile tilapia (Oreochromis niloticus) fingerlings. *Comp. Biochem. Physiol. Part C: Toxicol. Pharmacol.* 247, 109068. doi: 10.1016/j.cbpc.2021.109068

Meehan, T. L., Serizier, S. B., Kleinsorge, S. E., and McCall, K. (2016). Analysis of phagocytosis in the drosophila ovary. *Methods Mol. Biol.* 1457, 79–95. doi: 10.1007/978-1-4939-3795-0_6

Mohammadi, M. A., Cheng, Y., Aslam, M., Jakada, B. H., Wai, M. H., Ye, K. Z., et al. (2021). ROS and oxidative response systems in plants under biotic and abiotic stresses: revisiting the crucial role of phosphite triggered plants defense response. *Front. Microbiol.* 12, 631318. doi: 10.3389/fmicb.2021.631318

Mufeed, J., Ewadh, M., Ayyash, M. A., and Ewadh, H. (2018). Estimate GSH-Px and GST in benzene treated mice. *Biochem. Cell. Arch.* 18, 1037–1041.

Parker, K. S., El, N., Buldo, E. C., and MacCormack, T. J. (2024). Mechanisms of PVP-functionalized silver nanoparticle toxicity in fish: Intravascular exposure disrupts cardiac pacemaker function and inhibits Na^+/K^+-ATPase activity in heart, but not gill. *Comp. Biochem. Physiol. Part C: Toxicol. Pharmacol.* 277, 109837. doi: 10.1016/j.cbpc.2024.109837

Penninckx, M. J., and Jaspers, C. J. (1993). Metabolism and functions of glutathione in micro-organisms. *Adv. Microbial Physiol.* 34, 239–301. doi: 10.1016/S0065-2911(08)60031-4

Pu, G. Z., Wang, K. Y., Chen, X. X., Zeng, D. J., Mo, L., Liao, J. X., et al. (2021). Research progress on source, Transformation and eco-toxicological effect of silver nanoparticles in aquatic environment:A review. *Guangxi Sci.* 28, 363–372.

Qu, R., Chen, M., Liu, J., Xie, Q. T., Liu, N., and Ge, F. (2023). Blockage of ATPase-mediated energy supply inducing metabolic disturbances in algal cells under silver nanoparticles stress. *J. Environ. Sci.* 131, 141–150. doi: 10.1016/j.jes.2022.10.029

Subaramaniyam, U., Allimuthu, R. S., Vappu, S., Ramalingam, D., Balan, R., Paital, B., et al. (2023). Effects of mMicroplastics, and pesticides and nano-materials on fish health, oxidative stress and antioxidant defense mechanism. *Front. Physiol.* 14, 1217666. doi: 10.3389/fphys.2023.1217666

Tortella, G., Rubilar, O., Pieretti, J. C., Fincheira, P., Santana, B. D. M., Baldo, M. A. F., et al. (2023). Nanoparticles as a promising strategy to mitigate biotic stress in agriculture. *Antibiotics* 12, 338. doi: 10.3390/antibiotics12020338

Vicari, T., Dagostim, A. C., Klingelfus, T., Galvan, G. L., Monteiro, P. S., Pereira, L. D. S., et al. (2018). Co-exposure to titanium dioxide nanoparticles ($NpTiO_2$) and lead at environmentally relevant concentrations in the Neotropical fish species Hoplias intermedius. *Toxicology Reports* 2018 (5), 2214–7500. doi: 10.1016/j.toxrep.2018.09.001

Lu, X. R., Feng, X. L., Liu, C. Y., and Li, Q. (2018). Impact of Migration and Transformation of AgNPs on its Toxicity towards Environmental Microorganism. *Asian J. Ecotoxicolog* 13, 49–57.

Yue, W. P. (2010). Development prospect of Phaeodactylum triconutum as feed protein resource. *Hebei Fisheries* 12), 13–14 + 51.

Zhao, X. Y. (2018). Classification and physical properties of nanomaterials. *Inf. Recording Materials* 19, 20–21.

Zheng, G. J., and Wang, P. F. (2021). Research progress on toxic effects of nano silver in water environment. *Int. J. Ecol.* 10, 430–434. doi: 10.12677/IJE.2021.103048

Zong, P., Liu, Y., Chen, H., Fan, J. T., Wang, S. P., Wang, P. Y., et al. (2022). Inhibitory mechanism of nano-copper carbon composite on Microcystis aeruginosa. *Algal Res.* 68, 102877. doi: 10.1016/j.algal.2022.102877